IEEE Access
Multidisciplinary ⋮ Rapid Review ⋮ Open Access Journal

SPECIAL SECTION ON OPTICAL WIRELESS TECHNOLOGIES FOR 5G COMMUNICATIONS AND BEYOND

Received September 18, 2017, accepted October 30, 2017, date of publication November 13, 2017, date of current version December 5, 2017.

*Digital Object Identifier 10.1109/ACCESS.2017.2771333*

# Link Adaptation for MIMO OFDM Visible Light Communication Systems

**OMER NARMANLIOGLU[1], (Student Member, IEEE), REFIK CAGLAR KIZILIRMAK[2], (Member, IEEE), TUNCER BAYKAS[3], (Member, IEEE), AND MURAT UYSAL[1], (Senior Member, IEEE)**

[1]Department of Electrical and Electronics Engineering, Özyeğin University, 34794 Istanbul, Turkey
[2]Department of Electrical and Electronics Engineering, Nazarbayev University, 010000 Astana, Kazakhstan
[3]Department of Computer Engineering, Istanbul Medipol University, 34810 Istanbul, Turkey

Corresponding author: Refik Caglar Kizilirmak (refik.kizilirmak@nu.edu.kz)

The work of R. C. Kizilirmak was supported by the research grant from Nazarbayev University. The work of M. Uysal was supported by the Turkish Scientific and Research Council (TUBITAK) under Grant 215E311.

**ABSTRACT** In this paper, we investigate link adaptation for an orthogonal frequency division multiplexing (OFDM)-based multiple-input multiple-output (MIMO) visible light communication (VLC) system. The proposed adaptive OFDM VLC system supports both repetition coding (RC) and spatial multiplexing (SM) as MIMO modes and allows spatial mode switching based on channel conditions. Regarding to the instantaneous signal-to-noise ratio for both RC and SM modes, the maximum constellation size that can be supported for each MIMO mode on each subcarrier is determined. The MIMO mode that gives the highest spectral efficiency (SE) is then selected. The proposed joint MIMO mode selection and bit loading scheme maximizes the SE while satisfying a target bit error rate. Our numerical results reveal that a peak data rate up to 18.3 Gb/sec can be achieved in a $16 \times 16$ MIMO setting using light emitting diodes with cut-off frequency of 10 MHz in typical indoor environments.

**INDEX TERMS** Visible light communication, OFDM, adaptive transmission, bit loading, MIMO mode switching.

## I. INTRODUCTION

Visible light communication (VLC) is a short range wireless communication technology that uses the existing illumination infrastructure for data transmission [1]. VLC relies on intensity modulation and direct detection (IM/DD) where the information is encoded in the intensity of light and then recovered at the receiver with a photodetector (PD). In IM/DD, the information waveform that modulates the light intensity must be non-negative and real valued. In order to satisfy these conditions, earlier works on VLC have considered simple modulation techniques such as on-off keying (OOK) and pulse position modulation (PPM) [2].

To boost data rates over frequency-selective VLC channels, more recent works have adopted multicarrier transmission [3]–[7], particularly orthogonal frequency-division multiplexing (OFDM). The upcoming VLC standard IEEE 802.15.7m[1] that targets a peak data rate of 10 Gbit/sec [8] is also expected to adopt OFDM [9], [10]. In order to achieve such ambitious data rates, other techniques such as *adaptive transmission* and *multiple input multiple output (MIMO)* techniques should be further considered in conjunction with OFDM [11].

For indoor VLC systems, MIMO communications [12]–[17] can easily be realized through the deployment of multiple light sources which are readily available in most indoor spaces. In [12], a comparative performance evaluation of MIMO techniques, namely repetition coding (RC), spatial multiplexing (SM) and spatial modulation (SMOD) are presented for single-carrier VLC systems under the assumption of frequency-flat channels. In [13], the performance of SM is investigated using sub-optimal receiver techniques such as zero-forcing (ZF) and minimum mean square error (MMSE) and the effect of channel correlation is discussed. In [14], SM is considered and joint optimization of pre-coder and equalizer are studied for MIMO VLC systems. In [15], a power-efficient constellation design technique for MIMO VLC systems is proposed and

[1]The IEEE Task Group ‘‘Short Range Optical Wireless Communication’’ was originally named as 802.15.7r1. As of September 2016, it was renamed as 802.15.7m.

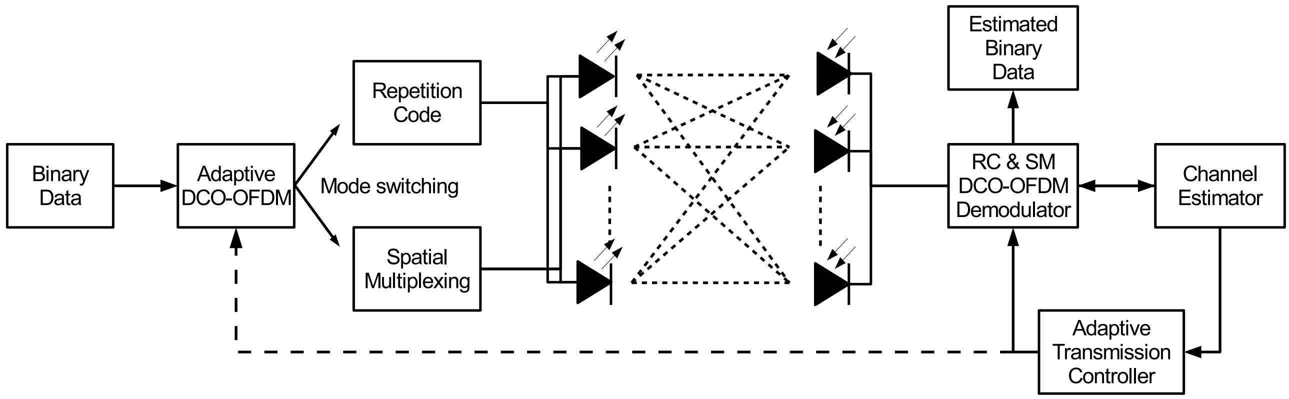


**FIGURE 1. Block diagram of the proposed adaptive MIMO OFDM VLC system.**

compared with RC, SM and SMOD. In [16], the combination of MIMO and OFDM is considered and performance comparison among RC, SM and SMOD techniques is presented for multi-carrier VLC systems. In [17], pre-coder design for a multi-user MIMO OFDM system is investigated.

Adaptive transmission, also known as link adaptation, refers to the selection of transmission parameters such as modulation size, transmit power etc. according to the channel conditions. Adaptive transmission has been extensively studied in the context of radio frequency (RF) communications and recently applied to VLC systems. Particularly, OFDM-based adaptive VLC systems have been explored in [18]–[20] where bit and power loading are considered. Link adaptation for coded OFDM VLC systems is further studied in [21] where code rate and modulation order are selected as adaptive transmission parameters.

Link adaptation for MIMO VLC systems has also attracted some attention [22], [23]. In [22], a MIMO system utilizing SM technique is considered and optimal power control and modulation selection scheme are studied. In [23], a transmitter/receiver selection algorithm is proposed for MIMO VLC systems with SMOD. It should be noted that the works in [22] and [23] are mainly limited to single-carrier architectures. To the best of our knowledge, the only existing work on adaptive MIMO OFDM VLC systems is [24] where SM is considered and the performance improvements through bit and power loading are presented.

In this work, we revisit the design of adaptive MIMO OFDM VLC system. Unlike [24] where the system architecture is built on a specific MIMO technique, we further consider spatial dimension as an adaptation parameter. The proposed adaptive OFDM VLC system supports both RC and SM modes and allows MIMO mode switching based on channel conditions. Specifically, we propose a joint MIMO mode selection and bit loading scheme to maximize the spectral efficiency (SE) while satisfying a given bit-error-rate (BER) target. Our results reveal that a peak data rate up to 18.3 Gbits/sec can be achieved in a $16 \times 16$ MIMO setting under realistic indoor channel conditions.

The remainder of this work is organized as follows. In Section II, we present MIMO OFDM VLC system model. In Section III, we present numerical results and finally conclude in Section IV.

*Notation:* $(.)^*$, $[.]^{\mathrm{T}}$, $[.]^{\mathrm{H}}$ and $||.||^2$ denote complex conjugate, transpose, Hermitian and Euclidean distance operations. $F\{.\}$ represents the continuous Fourier transform and $Q(.)$ is the tail probability of standard normal distribution. $\lceil x \rceil$ rounds $x$ to the nearest integer greater than or equal $x$. Vectors are denoted by bold face regular letters, e.g., $\mathbf{X}$. $X[k]$ denotes the $k^{th}$ element of $\mathbf{X}$.

## II. SYSTEM MODEL

We consider a MIMO system with $L$ light emitting diode (LED) luminaries and $P$ PDs (see Fig. 1). The proposed adaptive MIMO system supports two different MIMO modes. In RC mode, all the LEDs emit the same information to extract diversity gain through repetition. In SM mode, each LED emits different information to extract multiplexing gain. Based on the channel conditions, our adaptive scheme selects the MIMO mode and modulation order per subcarrier.

### A. MIMO OFDM TRANSMISSION

The system architecture is built upon direct current biased optical OFDM (DCO-OFDM). In DCO-OFDM, binary information is first mapped to complex symbols using either $M-$ary phase-shift keying (PSK) or quadrature amplitude modulation (QAM) with the average symbol energy $E$. Assume that $N$ is the number of subcarriers. Let $s_{l,1}$ $s_{l,2}$ $\ldots$ $s_{l,N/2-1}$ denote the complex-valued modulated symbol sequence to be transmitted from the $l^{th}$ LED. To ensure that the output of inverse discrete Fourier transform (IDFT) is real valued, Hermitian symmetry is imposed resulting in the transmitted sequence of $\mathbf{X}_l = \left[0\ s_1\ s_2\ \ldots\ s_{N/2-1}\ 0\ s^*_{N/2-1}\ \ldots\ s^*_2\ s^*_1\right]^{\mathrm{T}}$. The IDFT output is $\mathbf{x}_l$ whose $n^{th}$ element is written as

$$x_l[n] = \frac{1}{\sqrt{N}} \sum_{k=0}^{N-1} X_l[k] e^{j\frac{2\pi nk}{N}}, \quad n \in \{0, 1, \ldots, N-1\}. \quad (1)$$

The imposed Hermitian symmetry ensures that $x_l[n]$ is real valued. A cyclic prefix with the length of $N_{CP}$ is appended to $\mathbf{x}_l$ in order to compensate the intersymbol interference (ISI). Finally, a DC bias, $B_{DC}$, is applied to shift the amplitude values to the dynamic range of the LEDs. The resulting signals then propagate through the optical channel to the PDs.

The received signal by each PD is first sampled at a rate of $T_S$ and then discrete Fourier transform (DFT) is performed to obtain the frequency domain signal. The output of DFT at the $p^{th}$ PD on the $k^{th}$ subcarrier can be written as

$$Y_p[k] = \sqrt{\frac{E}{L}} R \sum_{l=1}^{L} X_l[k] H_{p,l}[k] + V_p[k], \tag{2}$$

where $R$ is PD responsivity (A/W) and $V_p[k]$ is additive white Gaussian noise (AWGN) term with zero mean and $N_0B$ variance. Here, $N_0$ denotes noise power spectral density (PSD) and $B = 1/2T_S$ is system bandwidth at Nyquist rate. In (2), total electrical information energy is shared among $L$ LEDs in order to maintain the same average electrical transmitted signal energy for different configurations. In (2), $H_{p,l}[k]$ is the DFT response of the band-limited electrical channel impulse response (CIR) between the $l^{th}$ LED and the $p^{th}$ PD, i.e., $H_{p,l}(f) = G_T(f)H^{\mathrm{E2E}}_{p,l}(f)G_R(f)$ where $G_T(f) = F\{g_T(t)\}$ and $G_R(f) = F\{g_R(t)\}$ respectively denote transmit and receive filter frequency responses and $H^{\mathrm{E2E}}_{p,l}(f)$ is the end-to-end channel frequency response between the $l^{th}$ LED and the $p^{th}$ including optical CIR and low-pass filter characteristics of receiver front-end.

### *B. MIMO MODES*

As earlier mentioned, the proposed scheme allows selection between two different MIMO modes. In RC mode, the same information is transmitted from each LED. Therefore, the transmitted sequences are identical, i.e., $X_1[k] = X_2[k] = \ldots = X_L[k] = X[k]$. If perfect channel state information is available at the receiver, the Maximum Likelihood (ML) decision rule is given by

$$\hat{X}[k] = \underset{X[k]\in\Omega_k}{\arg\min} \left[ \sum_{p=1}^{P} \left\| Y_p[k] - X[k]R\sum_{l=1}^{L} H_{p,l}[k] \right\|^2 \right], \tag{3}$$

where $\Omega_k$ is the set of constellation points on $k^{th}$ subcarrier.

In SM mode,[2] we use ZF receiver.[3] The ZF receiver multiplies the received signal with the pseudo-inverse of $\mathbf{H}[k]$ which can be written as $\mathbf{W}[k] = \left(\mathbf{H}^{\mathrm{H}}[k]\mathbf{H}[k]\right)^{-1}\mathbf{H}^{\mathrm{H}}[k]$ and then the equalized signal becomes $\tilde{\mathbf{Y}}[k] = \mathbf{W}[k]\mathbf{Y}[k]$. Finally, the decision is made based on

$$\hat{X}_l[k] = \underset{X_l[k]\in\Omega_{l,k}}{\arg\min} \left[ \tilde{Y}_l[k] - X_l[k]R \right], \quad l \in \{1, 2 \ldots L\}, \tag{4}$$

[2]It should be noted that for SM mode, $P$ should be equal to or greater than $L$.

[3]Although ML decoder is optimal, it requires an exhaustive search among $M^L$ options which might be computationally prohibitive.

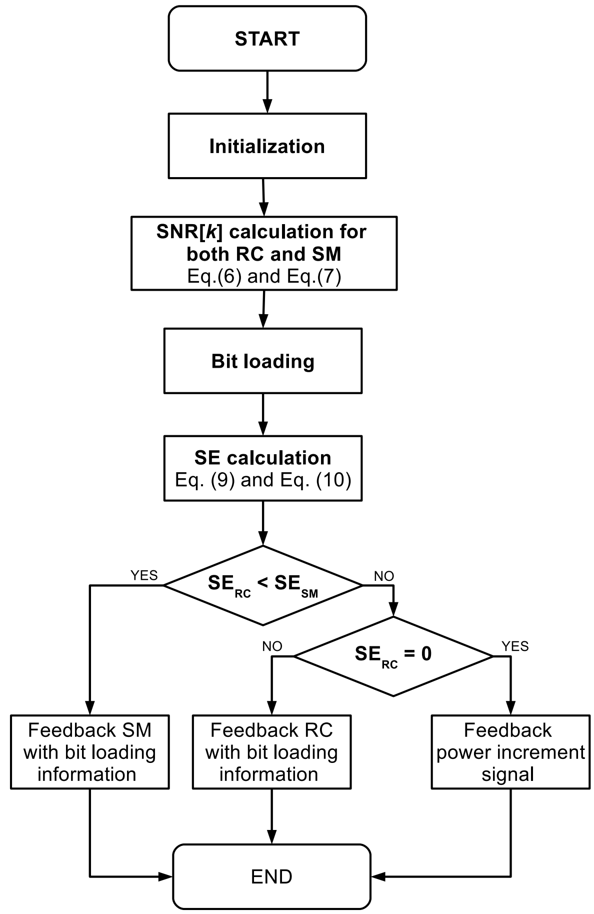


**FIGURE 2. Flowchart of the proposed algorithm.**

where $\Omega_{l,k}$ is the set of constellation points on $l^{th}$ subchannel (independent parallel paths between LEDs and PDs after ZF equalization) and $k^{th}$ subcarrier.

### *C. LINK ADAPTATION ALGORITHM*

For the MIMO OFDM VLC system under consideration, the receiver first calculates the instantaneous signal-to-noise ratio (SNR) per subcarrier for both RC and SM modes. The receiver then determines the maximum constellation size on each subcarrier that can be supported for each MIMO mode while satisfying a predefined target BER. The receiver selects the MIMO mode that provides the highest SE. The flowchart of the proposed technique is presented in Fig. 2 and the bit loading step is further detailed in Algorithm 1.

For RC mode, SNR available at the output of ML receiver and for SM mode, SNR at the output of ZF are used. Specifically, for RC mode, the SNR for the $k^{th}$ subcarrier is given by

$$\mathrm{SNR_{RC}}[k] = \frac{ER^2}{LN_0B} \sum_{p=1}^{P} \left| \sum_{l=1}^{L} H_{p,l}[k] \right|^2. \tag{6}$$

For SM mode, the SNR at the output of the equalizer on the $k^{th}$ subcarrier and the $l^{th}$ subchannel is obtained as

$$\mathrm{SNR_{SM_l}}[k] = \frac{ER^2}{LN_0B\sum_{p=1}^{P}\left|W_{l,p}[k]\right|^2}. \tag{7}$$

Subcarrier-based BER for different constellations can be calculated as in (5) given at the bottom of the page [25]. Required SNR levels to achieve a predefined BER target can be obtained by taking the inverse of (5). For instance, for 2−PSK and square $M$-QAM, we can directly calculate it by

$$\mathrm{SNR}[k]=\begin{cases}0.5Q^{-2}\left(\mathrm{BER}[k]\right), & 2-\mathrm{PSK}\\ \frac{M-1}{3}Q^{-2}\left(\frac{\sqrt{M}\log_2\sqrt{M}\mathrm{BER}[k]}{2\left(\sqrt{M}-1\right)}\right), & M-\ \mathrm{QAM}\,.\end{cases} \tag{8}$$

For rectangular $M=U\times J$ QAM, the inverse is not available in closed-form, but can be easily calculated through numerical means.

**Algorithm 1** Pseudo-Code of Bit Loading Mechanism

```
Set each element of D_RC and D_SM to one;
for each k in {1, 2, ... N/2 − 1} do
    for each modulation order in given set do
        if SNR_RC[k] ≥ required SNR to satisfy given
        BER target then
            Set D_RC[k] with this modulation order;
        for each l in {1, 2, ... L} do
            if SNR_SM_l[k] ≥ required SNR to satisfy
            given BER target then
                Set D_SM_l[k] with this modulation order;
```

As an example, assume that a BER of $10^{-5}$ is targeted. Based on (8), the required receive SNR levels for different modulation sizes are obtained and provided in a look-up table (LUT) (see Table 1). We consider the modulation sizes up to 4096−QAM that is being considered for DCO-OFDM in ongoing standardization work of VLC [26].

From this LUT, the subcarrier-based maximum constellation sizes that can be supported for RC and SM modes are determined. Let $D_{\mathrm{RC}}[k]$ denote the maximum constellation size on the $k^{th}$ subcarrier for RC mode. Similarly, for SM mode, let $D_{\mathrm{SM}_l}[k]$ denote the maximum constellation size that can be supported on the $k^{th}$ subcarrier and $l^{th}$ subchannel. The corresponding SEs for RC and SM modes are then respectively calculated as

$$\mathrm{SE}_{\mathrm{RC}}=\frac{1}{N+N_{CP}}\sum_{k=1}^{N/2-1}\log_2\ D_{\mathrm{RC}}[k]\ \mathrm{bits/sec/Hz}, \tag{9}$$

**TABLE 1.** LUT for target BER of $10^{-5}$.

| Modulation | Required receive SNR [dB] |
|---|---|
| 2−PSK | 9.59 |
| 4−QAM | 12.60 |
| 8−QAM | 17.29 |
| 16−QAM | 19.46 |
| 32−QAM | 23.54 |
| 64−QAM | 25.57 |
| 128−QAM | 29.53 |
| 256−QAM | 31.53 |
| 512−QAM | 35.47 |
| 1024−QAM | 37.47 |
| 2048−QAM | 41.41 |
| 4096−QAM | 43.41 |

**TABLE 2.** Feedback data frame structure.

| Transmission Mode | $1^{\mathrm{st}}$ subcarrier | $2^{\mathrm{nd}}$ subcarrier | ... ... | $[N/2-1]^{\mathrm{th}}$ subcarrier |
|---|---|---|---|---|
| 2 bits | $\mathcal{B}$ bits | $\mathcal{B}$ bits | ... | $\mathcal{B}$ bits |

$$\mathrm{SE}_{\mathrm{SM}}=\frac{1}{N+N_{CP}}\sum_{l=1}^{L}\sum_{k=1}^{N/2-1}\log_2\ D_{\mathrm{SM}_l}[k]\ \mathrm{bits/sec/Hz}. \tag{10}$$

Based on (9) and (10), the receiver selects either RC or SM as the MIMO mode to give the highest SE. The corresponding data rate is equal to $\mathrm{SE}/T_S$ [bits/sec]. Selected MIMO mode and related bit loading information (i.e., constellation size for each subcarrier) is sent to the transmitter through a feedback link. It should be noted that SNR level may not be sufficient for the target BER with neither RC nor SM modes. In this case, power increment signal is transmitted through feedback link to ensure that the transmission starts and then the process of MIMO mode and modulation order selection per subcarrier is repeated.

### D. FEEDBACK LINK

The proposed adaptive MIMO OFDM relies on a feedback link that conveys selected MIMO mode and related bit loading information (i.e., constellation size for each subcarrier) to the transmitter. In the literature, uplink for VLC systems is usually supported by the use of RF, infrared or wavelength division technologies (e.g., [27]–[29]). The required packet structure for the feedback information is shown in Table 2. The first two bits represent the transmission mode, i.e., "00" denotes RC and "01" denotes SM. "10", on the other hand,

$$\mathrm{BER}[k]\approx\begin{cases}Q\left(\sqrt{2\mathrm{SNR}[k]}\right), & 2\text{ - PSK}\\ \frac{2\left(\sqrt{M}-1\right)}{\sqrt{M}\log_2\sqrt{M}}Q\left(\sqrt{\frac{3\mathrm{SNR}[k]}{M-1}}\right), & \text{square } M-\mathrm{QAM}\\ \frac{2}{\log_2\left(U\times J\right)}\left[\frac{U-1}{U}Q\left(\sqrt{\frac{6\mathrm{SNR}[k]}{U^2+J^2-2}}\right)+\frac{J-1}{J}Q\left(\sqrt{\frac{6\mathrm{SNR}[k]}{U^2+J^2-2}}\right)\right], & \text{rectangular } M=U\times J-\mathrm{QAM}\end{cases} \tag{5}$$

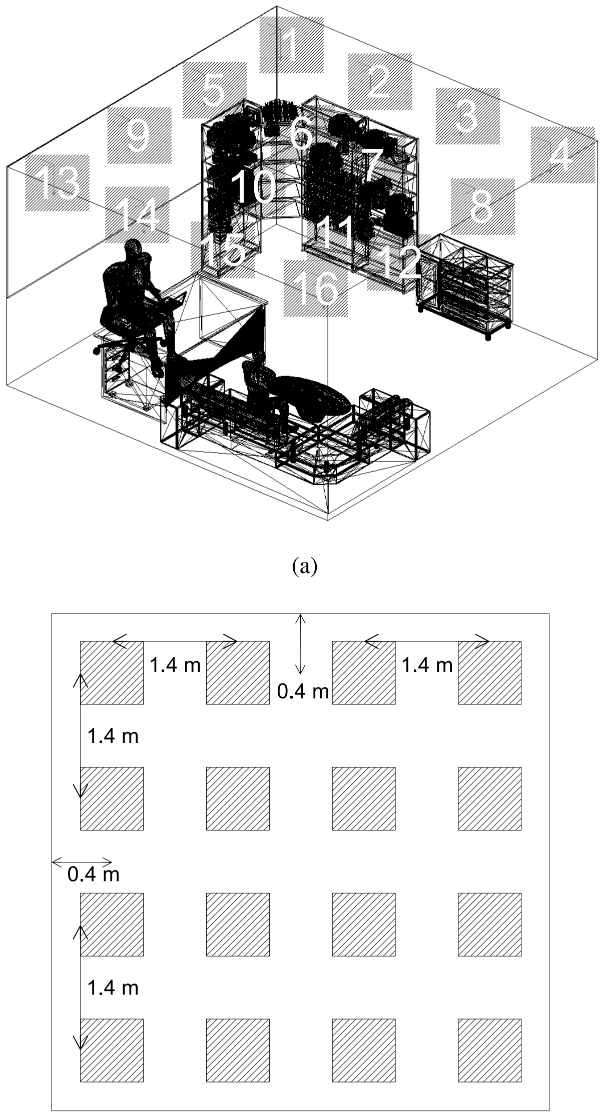


(a)

(b)

**FIGURE 3. (a) Top view of the office space, (b) arrangement of luminaries.**

indicates power increment signal. The following bits represent the deployed modulation order on each subcarrier. $\mathcal{B}$ is equal to $\lceil \log_2(O_M) \rceil$ and $O_M$ is the total number of available modulation orders. In the case of $O_M = 12$ different modulation orders as in Table 1 (i.e., 2−PSK, 4−QAM, ...4096−QAM), $\mathcal{B}$ becomes 4 bits. If the total number of subcarriers $N = 1024$, the feedback information becomes 2046 bits.

## III. RESULTS AND DISCUSSIONS

In this section, we present the performance of our proposed adaptive MIMO OFDM VLC system.

### A. INDOOR CHANNEL MODEL AND SIMULATION SETUP

We consider an office space with dimensions of 5 m × 5 m × 3 m (see Fig. 3a) and 16 LED ceiling light sources (see Fig. 3b). For typical indoor scenarios, the Illuminating Engineering Society of North America (IES) Standard [30] suggests surface illumination levels between 100 lux and 1000 lux. The illumination level depends on the properties of luminary (i.e., lighting output) as well as the arrangement of luminaries (i.e., number of luminaries, intra-distance, etc). In our case, we consider 17 W for each LED. This achieves illumination levels in the range of 365 − 612 lux complying with the IES standard. Note that for DCO-OFDM systems, the brightness is controlled with the bias voltage $B_{DC}$ that neither conveys information nor affects the SNR at the receiver [31], [32].

The destination terminal is in the form of a laptop computer placed on the desk. It is connected to four USB hubs each of which is equipped with 4 PDs (see Fig. 4). We further consider different PD separations within a hub. Specifically, the separation between adjacent PDs, each with a surface area of 0.07 cm$^2$ (e.g., [33]), is taken as 1 cm, 3 cm and 5 cm. The distance between adjacent USB hubs is set at 12.5 cm. The other specifications are summarized in Table 3.

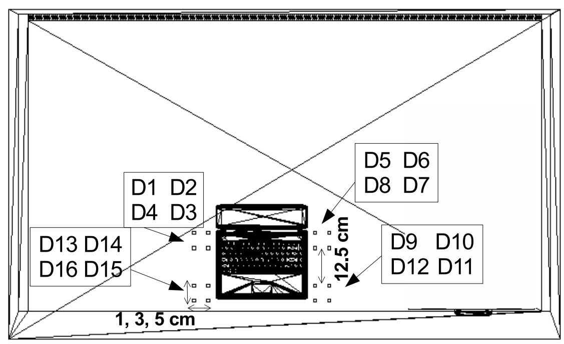


**FIGURE 4. Top view of the desk with laptop computer and PDs labeled from 1 to 16.**

Let $h^{\text{opt}}_{p,l}(t)$, $l \in \{1, 2 \ldots L\}$, $p \in \{1, 2 \ldots P\}$ denote optical CIR for the link from the $l^{th}$ LED to the $p^{th}$ PD. Optical CIRs for each link are obtained using ray tracing simulations similar to those in [34]. As an example, we present the CIRs for the first PD, i.e., $h^{\text{opt}}_{1,l}(t)$, $l \in \{1, 2, \ldots 16\}$ in Fig. 5. In addition to the multipath propagation environment, the low-pass filter nature of the LEDs should be further taken into account. The frequency response of LED is commonly modelled as [35]

$$H_{\text{LED}}(f) = \frac{1}{1 + j\frac{f}{f_{\text{cut-off}}}}, \tag{11}$$

where $f_{\text{cut-off}}$ is the LED 3−dB cut-off frequency. In order to extend typical modulation bandwidth (e.g., 2 − 3 MHz) of commercial white LR24-38SKA35 LED, blue filtering is applied at the receiver with a drawback of reducing the received optical power by %50 [36]. The end−to−end channel frequency response taking into account the LED characteristics can be then expressed as $H^{\text{E2E}}_{p,l}(f) = H_{\text{LED}}(f) H^{\text{opt}}_{p,l}(f)$ where $H^{\text{opt}}_{p,l}(f) = F\{h^{\text{opt}}_{p,l}(t)\}$.

In our simulation study, we consider 4 × 4, 4 × 16 and 16 × 16 MIMO scenarios (see Table 4). System parameters

**TABLE 3. Office room model specifications.**

| | |
|---|---|
| **Room size** | 5 m × 5 m × 3 m |
| **Materials** | Walls: Plaster, Ceiling: Plaster, Floor: Pinewood, Desk: Pinewood |
| **Objects** | 1 desk and a chair paired with desk, 1 laptop on the desk, 1 desk light on the desk, 1 library, 1 couch, 1 coffee table, window, 2 human bodies |
| **Object specifications** | Desk: Pinewood (Height 0.88 m), Chair: Black gloss paint, Laptop: Black gloss paint<br>Desk light: Black gloss paint, Library: Pinewood, Window: Glass<br>Couch: Cotton, Coffee table: Pinewood<br>Human body: Head & Hands (assumed to be absorbing), clothes (cotton), shoes (black gloss) |
| **Luminary Specifications** | 17 Watt<br>Brand: LR24-38SKA35 Cree Inc.<br>Half viewing angle: 40° |

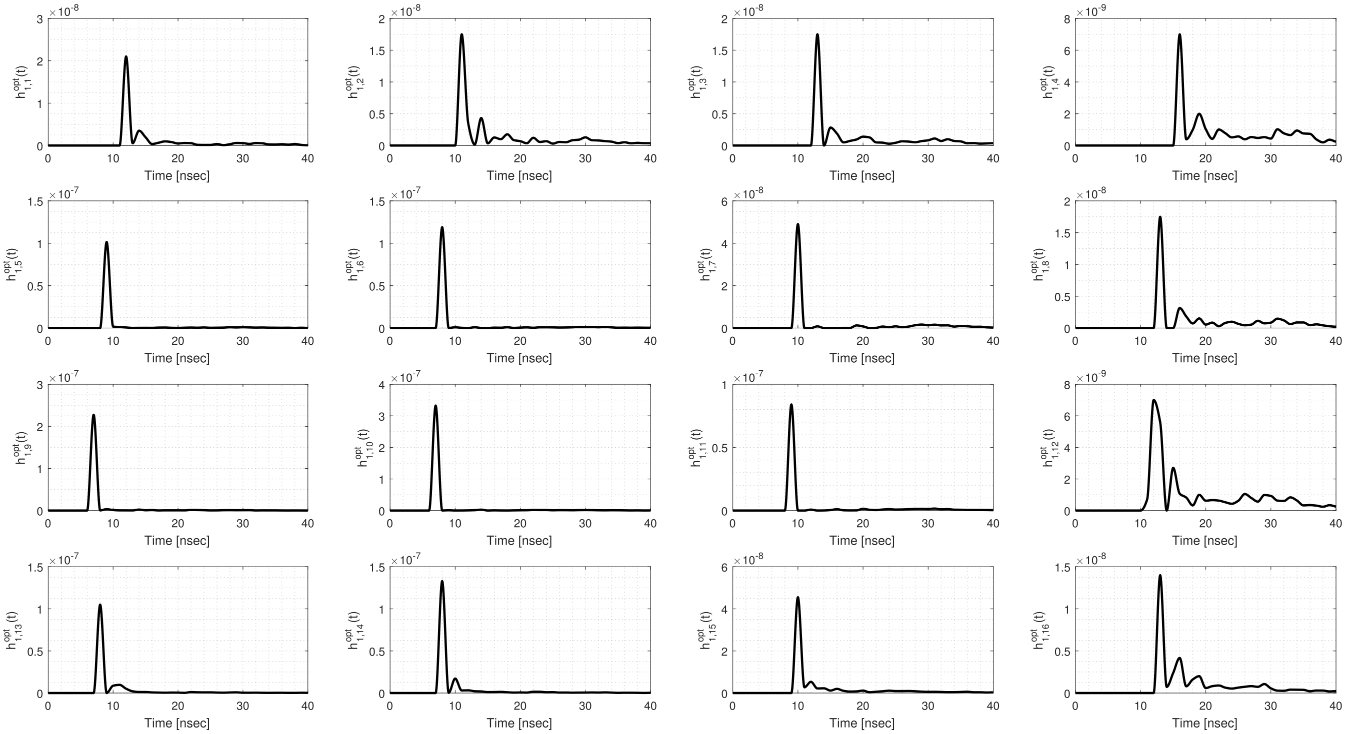

**FIGURE 5. Optical CIRs for the first PD.**

**TABLE 4. Different MIMO scenarios under consideration.**

| | MIMO Configuration | LEDs | PDs |
|---|---|---|---|
| **Scenario I** | 16 × 16 | ALL | ALL |
| **Scenario II** | 4 × 4 | 1 4 13 16 | 1 5 11 16 |
| **Scenario III** | 4 × 4 | 6 7 10 11 | 1 2 3 4 |
| **Scenario IV** | 4 × 16 | 1 4 13 16 | ALL |

are summarized in Table 5. In Scenario I, we have a 16 × 16 MIMO system where all LEDs in the room and all PDs attached to the destination terminal are used for data transmission. In Scenario II, we consider a 4 × 4 MIMO system where the LEDs indexed by 1, 4, 13 and 16 and PDs indexed by 1, 5, 11, 16 (one from each hub) are used for data transmission. In 4 × 4 MIMO system considered in Scenario III, LEDs indexed by 6, 7, 10, 11 and PDs indexed by 1, 2, 3, 4 are assumed to be active. It can be noted that the intra-distances between LEDs/PDs are smaller in Scenario III in comparison to Scenario II. Furthermore, we consider a 4 × 16 MIMO system to investigate the impact of receive diversity in Scenario IV. It should be emphasized that in all four scenarios under consideration, all LEDs are always on and used for illumination. The above scenarios describe LEDs and PDs which are only used for data transmission/reception.

**TABLE 5. Simulation parameters.**

| | |
|---|---|
| Number of subcarriers ($N$) | 1024 |
| Cyclic prefix length ($N_{CP}$) | 48 |
| Pulse shape filter ($g_T(t), g_R(t)$) | Sinc filter |
| Sampling interval ($T_S$) | 5 nsec |
| Responsivity ($R$) | 0.28 A/W [36] |
| LED cut-off frequency ($f_{\text{cutt-off}}$) | 10 MHz |
| Bandwidth ($B$) | 100 MHz |
| Noise PSD ($N_0$) | $10^{-22}$ W/Hz [36] |
| Target BER | $10^{-5}$ |

### *B. NUMERICAL RESULTS*

In Fig. 6, SE and the corresponding data rate of the proposed algorithm (indicated by ·) are presented for

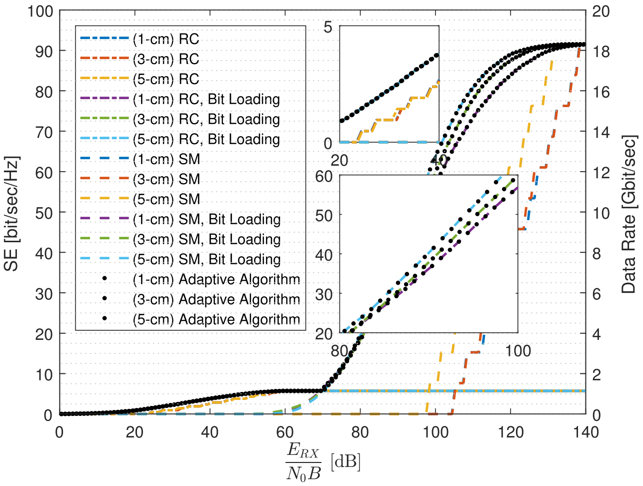


**FIGURE 6.** SE and data rate of the adaptive algorithm for Scenario I.

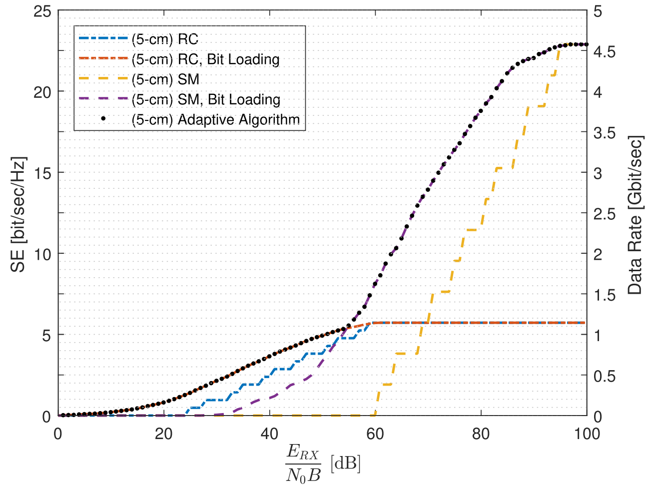


**FIGURE 7.** SE and data rate of the adaptive algorithm for Scenario II.

Scenario I. The results are given with respect to $E_{RX}/N_0B$ where $E_{RX} = \frac{ER^2}{L}\sum_{p=1}^{P}\left|\sum_{l=1}^{L} H_{p,l}[k]\right|^2$. As benchmarks, we consider stand-alone RC and SM systems with and without bit loading. When bit loading is not implemented, all subcarriers are modulated with the same modulation order. The highest possible modulation order is chosen based on the average BER among subcarriers and target BER. It can be observed that in low SNR region, RC outperforms SM as a result of diversity gains. Specifically, for $\frac{E_{RX}}{N_0B} < 69.37$ dB, it is observed that RC has better performance. At 69.37 dB, this trend reverses. After this point, SM significantly outperforms its counterpart taking advantage of the multiplexing gains. It should be also noted that the performance of RC saturates at 59.55 dB where all the subcarriers employ 4096−QAM. The maximum achievable SE with RC mode is 5.72 bits/sec/Hz and this corresponds to a data rate of 1.14 Gbits/sec. At 135.5 dB, SM saturates (in the case where adjacent PDs are separated by 5 cm) and maximum SE of 91.52 bits/sec/Hz (equivalent data rate of 18.3 Gbit/sec) is achieved. As observed from performance plots, the proposed algorithm benefits from both RC and SM through mode switching based on channel conditions and has a superior performance over stand-alone cases.

In the same figure, we also investigate the effect of PD separation. When the adjacent PDs are separated by 1 cm, SE of 76.35 bits/sec/Hz is achieved using SM with bit loading at the $E_{RX}/N_0B$ of 112.4 dB. This value increases to 81.08 bits/sec/Hz and 83.64 bits/sec/Hz when the PD separation is 3 cm and 5 cm, respectively. The impact of PD separation is more apparent for SM without bit loading. Numerically, 15.25, 22.88 and 38.13 bits/sec/Hz are obtained for 1 cm, 3 cm and 5 cm separation, respectively, at the same $E_{RX}/N_0B$ value of 112.4 dB. The increment is due to weaker channel correlation as a consequence of wider PD separation. When diversity is considered, SEs of 3.86, 3.864 and 3.871 bits/sec/Hz are achieved for the PD separations of 1 cm, 3 cm and 5 cm, respectively, at the $E_{RX}/N_0B$ of 40.37 dB. The differences are negligible and this is due to the fact that the path loss, instead of channel correlation, is the main factor which determines the diversity performance.

In Fig. 7, we present the performance of 4 × 4 MIMO system for Scenario II where one PD is selected from each hub. Similar to the previous scenario, our adaptive algorithm benefits from both MIMO modes in different SNR regions. When $E_{RX}/N_0B$ is less than 53.93 dB, adaptive algorithm selects RC mode. At the 53.93 dB, SE of 5.33 bits/sec/Hz is achieved. For $E_{RX}/N_0B$ values larger than 53.93 dB, SM outperforms RC in terms of SE and the proposed system switches to SM mode. When $E_{RX}/N_0B$ becomes 99.93 dB, all subcarriers are modulated with 4096−QAM symbols and a data rate of 4.58 Gbits/sec is achieved whereas RC achieves 1.14 Gbits/sec at this point. As compared to the 16 × 16 MIMO system (Scenario I), the $E_{RX}/N_0B$ range where 4 × 4 RC outperforms 4 × 4 SM is much smaller than the 16 × 16 MIMO system under consideration due to the fact that channel correlation is weaker as a result of the relatively larger space between active LEDs at the transmit side and PDs at the receive side. However, the data rate reduces from 18.3 Gbits/sec to 4.58 Gbits/sec since the multiplexing gain is determined by $\min\{L, P\} = 4$.

In Fig. 8, the performance results are provided for the 4 × 4 MIMO system of Scenario III. In this scenario, the PD separation is kept at 5 cm as in Scenario II, however, the correlations of the channel gains are higher than those in Scenario II due to the reduced distance between the LEDs and PDs. In this case, SM requires higher $E_{RX}/N_0B$ to satisfy the target BER due to higher correlation between the channel gains. Therefore, our adaptive algorithm switches to SM mode at higher $E_{RX}/N_0B$ value, 69.86 dB, with respect to Scenario II. On the other hand, RC satisfies the BER target with lower transmit power since higher channel gains as a result of better field-of-views (FOVs) and shorter distances between LEDs and PDs.

In Fig. 9, we present the performance results for 4 × 16 MIMO system in Scenario IV. As compared to Scenario II, RC and SM modes require less $E_{RX}/N_0B$ in order to start

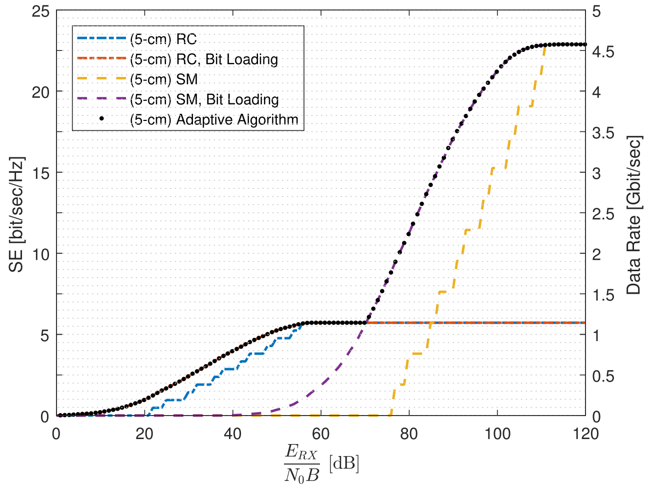


**FIGURE 8.** SE and data rate of the adaptive algorithm for Scenario III.

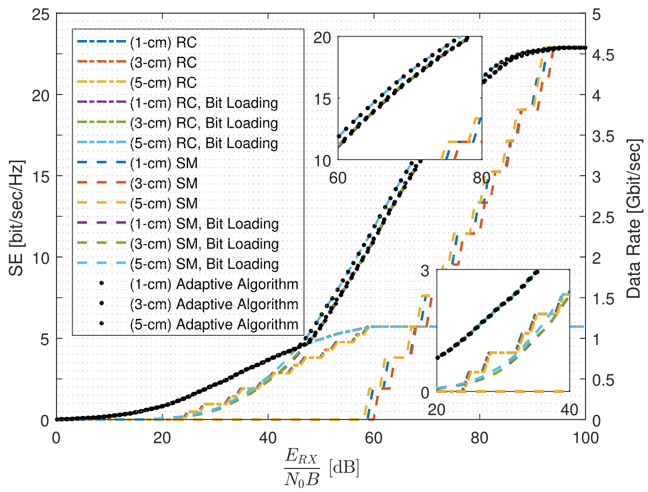


**FIGURE 9.** SE and data rate of the adaptive algorithm for Scenario IV.

transmission. This is due to the increased number of receivers, effectively providing diversity gains. This also leads earlier switching from RC mode to SM mode in adaptive transmission. Furthermore, we evaluate the effect of PD separation for this $4 \times 16$ MIMO system. It is observed that the effect of PD spacing within a hub is negligible. On one hand, they have an impact on multiplexing performance, however, the effect decreases since $4 \times 16$ MIMO system provides diversity gains.

It is also observed that stand-alone RC and SM systems with bit loading outperforms the systems without bit-loading. When bit loading is not implemented, all subcarriers are modulated with the same modulation order. The highest possible modulation order is chosen based on the average BER among subcarriers. As a result, achieved SEs are the same for particular $E_{RX}/N_0B$ range and increase gradually (step by step) as the transmit power increases.

## IV. CONCLUSION

In this paper, we have proposed an adaptive algorithm for MIMO OFDM VLC systems. The proposed algorithm was designed to maximize SE while satisfying a given BER target. Based on the channel conditions, it performs bit loading (i.e., selection of modulation size) and switches between RC and SM modes to extract either diversity or multiplexing gain. Our simulation results demonstrated data rates up to 18.3 Gbit/sec for a $16 \times 16$ MIMO system. We further investigated the effects of transmitter-receiver alignment and receiver diversity on the system performance. It was observed that weaker channel correlations lead performance improvement in the SM mode and that diversity provides additional performance gains on both types, especially in the RC mode.

## REFERENCES

[1] S. Arnon, J. Barry, G. Karagiannidis, R. Schober, and M. Uysal, Eds., *Advanced Optical Wireless Communication Systems*. Cambridge, U.K.: Cambridge Univ. Press, 2012.
[2] S. Rajagopal, R. D. Roberts, and S.-K. Lim, "IEEE 802.15.7 visible light communication: Modulation schemes and dimming support," *IEEE Commun. Mag.*, vol. 50, no. 3, pp. 72–82, Mar. 2012.
[3] J. Armstrong, "OFDM for optical communications," *J. Lightw. Technol.*, vol. 27, no. 3, pp. 189–204, Feb. 1, 2009.
[4] J. Armstrong and A. J. Lowery, "Power efficient optical OFDM," *Electron. Lett.*, vol. 42, no. 6, pp. 370–372, Mar. 2006.
[5] D. Tsonev, S. Sinanovic, and H. Haas, "Novel unipolar orthogonal frequency division multiplexing (U-OFDM) for optical wireless," in *Proc. IEEE 75th Veh. Technol. Conf. (VTC Spring)*, May 2012, pp. 1–5.
[6] N. Fernando, Y. Hong, and E. Viterbo, "Flip-OFDM for unipolar communication systems," *IEEE Trans. Commun.*, vol. 60, no. 12, pp. 3726–3733, Dec. 2012.
[7] D. Tsonev, S. Videv, and H. Haas, "Unlocking spectral efficiency in intensity modulation and direct detection systems," *IEEE J. Sel. Areas Commun.*, vol. 33, no. 9, pp. 1758–1770, Sep. 2015.
[8] *TG7r1 Technical Considerations Document*, document IEEE 802.15-15/0492r3, 2015, accessed: Jun. 10, 2017. [Online]. Available: https://mentor.ieee.org/802.15/dcn/15/15-15-0492-03-007a-technical-considerations-document.docx
[9] D. Tsonev and N. Serafimovski, *Low-Bandwidth LiFi PHY & MAC*, document IEEE 802.15-16/0363r0, 2016, accessed: Jun. 10, 2017. [Online]. Available: https://mentor.ieee.org/802.15/dcn/16/15-16-0363-00-007a-text-input-lifi-low-bandwidth-phy-and-mac-d0.docx
[10] V. Jungnickel, *High-Bandwidth PHY*, document IEEE 802.15-16/0356r0, 2016, accessed: Jun. 10, 2017. [Online]. Available: https://mentor.ieee.org/802.15/dcn/16/15-16-0356-00-007a-text-input-for-high-bandwidth-phy.docx
[11] M. Uysal, O. Narmanlioglu, T. Baykas, and R. Kizilirmak, *Adaptive MIMO OFDM PHY Proposal for IEEE 802.15.7r1*, document IEEE 802.15-16/0008r2, 2016, accessed: Jun. 10, 2017. [Online]. Available: https://mentor.ieee.org/802.15/dcn/16/15-16-0008-02-007a-adaptive-mimo-ofdm-phy-proposal-for-ieee802-15-7r1.pdf
[12] T. Fath and H. Haas, "Performance comparison of MIMO techniques for optical wireless communications in indoor environments," *IEEE Trans. Commun.*, vol. 61, no. 2, pp. 733–742, Feb. 2013.
[13] C. He, T. Q. Wang, and J. Armstrong, "Performance of optical receivers using photodetectors with different fields of view in a MIMO ACO-OFDM system," *J. Lightw. Technol.*, vol. 33, no. 23, pp. 4957–4967, Dec. 1, 2015.
[14] K. Ying, H. Qian, R. J. Baxley, and S. Yao, "Joint optimization of precoder and equalizer in MIMO VLC systems," *IEEE J. Sel. Areas Commun.*, vol. 33, no. 9, pp. 1949–1958, Sep. 2015.
[15] Y.-J. Zhu, W.-F. Liang, J.-K. Zhang, and Y.-Y. Zhang, "Space-collaborative constellation designs for MIMO indoor visible light communications," *IEEE Photon. Technol. Lett.*, vol. 27, no. 15, pp. 1667–1670, Aug. 1, 2015.
[16] M. O. Damen, O. Narmanlioglu, and M. Uysal, "Comparative performance evaluation of MIMO visible light communication systems," in *Proc. 24th Signal Process. Commun. Appl. Conf. (SIU)*, May 2016, pp. 525–528.
[17] Q. Wang, Z. Wang, and L. Dai, "Multiuser MIMO-OFDM for visible light communications," *IEEE Photon. J.*, vol. 7, no. 6, Dec. 2015, Art. no. 7904911.
[18] L. Wu, Z. Zhang, J. Dang, and H. Liu, "Adaptive modulation schemes for visible light communications," *J. Lightw. Technol.*, vol. 33, no. 1, pp. 117–125, Jan. 1, 2015.

[19] J. Vucic, C. Kottke, S. Nerreter, K.-D. Langer, and J. W. Walewski, "513 Mbit/s visible light communications link based on DMT-modulation of a white LED," *J. Lightw. Technol.*, vol. 28, no. 24, pp. 3512–3518, Dec. 15, 2010.

[20] P. W. Berenguer, V. Jungnickel, and J. K. Fischer, "The benefit of frequency-selective rate adaptation for optical wireless communications," in *Proc. 10th Int. Symp. Commun. Syst., Netw. Digit. Signal Process. (CSNDSP)*, Jul. 2016, pp. 1–6.

[21] M. Wang *et al.*, "Efficient coding modulation and seamless rate adaptation for visible light communications," *IEEE Wireless Commun.*, vol. 22, no. 2, pp. 86–93, Apr. 2015.

[22] K.-H. Park, Y.-C. Ko, and M.-S. Alouini, "On the power and offset allocation for rate adaptation of spatial multiplexing in optical wireless MIMO channels," *IEEE Trans. Commun.*, vol. 61, no. 4, pp. 1535–1543, Apr. 2013.

[23] P. F. Mmbaga, J. Thompson, and H. Haas, "Performance analysis of indoor diffuse VLC MIMO channels using angular diversity detectors," *J. Lightw. Technol.*, vol. 34, no. 4, pp. 1254–1266, Feb. 15, 2016.

[24] Y. Hong, T. Wu, and L.-K. Chen, "On the performance of adaptive MIMO-OFDM indoor visible light communications," *IEEE Photon. Technol. Lett.*, vol. 28, no. 8, pp. 907–910, Apr. 15, 2016.

[25] K. Cho and D. Yoon, "On the general BER expression of one- and two-dimensional amplitude modulations," *IEEE Trans. Commun.*, vol. 50, no. 7, pp. 1074–1080, Jul. 2002.

[26] N. Serafimovski and V. Jungnikel, *May IEEE802.15.13 Minutes*, document IEEE P802.15-17-0311-00-0013, accessed: Jun. 10, 2017. [Online]. Available: https://mentor.ieee.org/802.15/dcn/17/15-17-0311-00-0013-meeting-minutes-of-tg13-may-2017.docx

[27] S. Shao *et al.*, "An indoor hybrid WiFi-VLC Internet access system," in *Proc. IEEE 11th Int. Conf. Mobile Ad Hoc Sensor Syst. (MASS)*, Oct. 2014, pp. 569–574.

[28] M. T. Alresheedi, A. T. Hussein, and J. M. H. Elmirghani, "Uplink design in VLC systems with ir sources and beam steering," *IET Commun.*, vol. 11, no. 3, pp. 311–317, 2017.

[29] W. Yuanquan and C. Nan, "A high-speed bi-directional visible light communication system based on RGB-LED," *China Commun.*, vol. 11, no. 3, pp. 40–44, 2014.

[30] *Lighting of Indoor Work Places*, document ISO 8995:2002 CIE S 008/E:2001, International Standard, accessed: Jun. 10, 2017. [Online]. Available: https://www.iso.org/standard/28857.html

[31] Y. Yang, Z. Zeng, J. Cheng, and C. Guo, "Spatial dimming scheme for optical OFDM based visible light communication," *Opt. Express*, vol. 24, no. 26, pp. 30254–30263, 2016.

[32] T. D. C. Little and H. Elgala, "Adaptation of OFDM under visible light communications and illumination constraints," in *Proc. IEEE 48th Asilomar Conf. Signals, Syst. Comput.*, Nov. 2014, pp. 1739–1744.

[33] *Si APD S2384*. Accessed: Jun. 10, 2017. [Online]. Available: http://www.hamamatsu.com/jp/en/product/category/3100/4003/4110/S2384/index.html

[34] F. Miramirkhani and M. Uysal, "Channel modeling and characterization for visible light communications," *IEEE Photon. J.*, vol. 7, no. 6, Dec. 2015, Art. no. 7905616.

[35] L. Grobe and K.-D. Langer, "Block-based PAM with frequency domain equalization in visible light communications," in *Proc. IEEE Globecom Workshops (GC Wkshps)*, Dec. 2013, pp. 1070–1075.

[36] J. Grubor, S. Randel, K. D. Langer, and J. W. Walewski, "Broadband information broadcasting using LED-based interior lighting," *J. Lightw. Technol.*, vol. 26, no. 24, pp. 3883–3892, Dec. 15, 2008.


**OMER NARMANLIOGLU** received the B.Sc. degree from the Department of Electrical and Electronics Engineering, Bilkent University, Ankara, Turkey, in 2014, and the M.Sc. degree from Özyeğin University, Istanbul, Turkey, in 2016, where he is currently pursuing the Ph.D. degree. He is currently with P. I. Works. His research interests are the physical and link layer aspects of communication systems and software-defined networking paradigm for radio access, transmission, and packet core networks.

**REFIK CAGLAR KIZILIRMAK** (M'10) was born in Izmir, Turkey, in 1981. He received the B.Sc. and M.Sc. degrees in electrical and electronics engineering from Bilkent University, Ankara, Turkey, in 2004 and 2006, respectively, and the Ph.D. degree from Keio University, Yokohama, Japan, in 2010. He was with the Communications and Spectrum Management Research Center, Ankara, where he was involved in on several telecommunication and defense industry projects. He is currently with the faculty of Electrical and Electronics Engineering, Nazarbayev University, Astana, Kazakhstan. He was a recipient of the IEEE VTS Japan 2008 Young Researcher's Award.

**TUNCER BAYKAS** was an Expert Researcher with NICT, Japan, from 2007 to 2012. He has served as a Co-Editor and the Secretary for 802.15 TG3c, and he has contributed many standardization projects, including 802.22, 802.11af, and 1900.7. He is the Vice Director of the Centre of Excellence in Optical Wireless Communication Technologies and the Vice Chair of the 802.19 Wireless Coexistence Working Group. He contributed to the technical requirements document and the channel models of 802.15.7r1 standardization, which will enable visible light communication. He is currently an Assistant Professor and the Head of the Department of Computer Engineering with Istanbul Medipol University.

**MURAT UYSAL** received the B.Sc. and M.Sc. degrees in electronics and communication engineering from Istanbul Technical University, Istanbul, Turkey, in 1995 and 1998, respectively, and the Ph.D. degree in electrical engineering from Texas A&M University, College Station, TX, USA, in 2001. He is currently a Full Professor and the Chair of the Department of Electrical and Electronics Engineering with Özyeğin University, Istanbul. He also serves as the Founding Director of the Center of Excellence in Optical Wireless Communication Technologies. Prior to joining Özyeğin University, he was a tenured Associate Professor with the University of Waterloo, Canada, where he still holds an adjunct faculty position. He has authored some 290 journal and conference papers in his research topics and received more than 7500 citations. His research interests are in the broad areas of communication theory and signal processing with a particular emphasis on the physical-layer aspects of wireless communication systems in radio and optical frequency bands.

His distinctions include the Marsland Faculty Fellowship in 2004, the NSERC Discovery Accelerator Supplement Award in 2008, the University of Waterloo Engineering Research Excellence Award in 2010, the Turkish Academy of Sciences Distinguished Young Scientist Award in 2011, and the Ozyegin University Best Researcher Award in 2014. He currently serves on the editorial board of the IEEE Transactions on Wireless Communications. In the past, he was an Editor of the IEEE Transactions on Communications, the IEEE Transactions on Vehicular Technology, the IEEE Communications Letters, *Wireless Communications and Mobile Computing Journal*, and the *Transactions on Emerging Telecommunications Technologies*, and a Guest Editor of the IEEE Journal on Selected Areas in Communications Special Issues on Optical Wireless Communication (2009 and 2015). He was involved in the organization of several IEEE conferences at various levels. He served as the Chair of the Communication Theory Symposium of IEEE ICC 2007, the Chair of the Communications and Networking Symposium of IEEE CCECE 2008, the Chair of the Communication and Information Theory Symposium of IWCMC 2011, a TPC Co-Chair of the IEEE WCNC 2014, and the General Chair of the IEEE IWOW 2015. Over the years, he has served on the technical program committee of more than 100 international conferences and workshops in the communications area.